A novel design approach for estimation of extreme load responses of a 10-MW floating semi-submersible type wind turbine

Rajiv Balakrishna[1], Oleg Gaidai[2], Fang Wang[2*], Yihan Xing[1], Shuaishuai Wang[3]

[1]Department of Mechanical and Structural Engineering and Materials Science, University of Stavanger, Norway

[2]Shanghai Engineering Research Centre of Marine Renewable Energy, College of Engineering Science and Technology, Shanghai Ocean University, Shanghai, China

[3]Norwegian University of Science and Technology, Trondheim, Norway

[*]Corresponding author: wangfang@shou.edu.cn

Abstract

Offshore structures are constructed to withstand extreme wind and wave-induced loads, so studying these extreme loads is vital as it allows offshore structures, e.g., wind turbines, to be designed and operated with minimal disruption. A novel statistical model that is precise and meticulous will facilitate these extreme load values to be estimated accurately. Therefore, the recently developed bivariate average conditional exceedance rate (ACER2D) method is utilized in this paper. This multivariate statistical analysis is more appropriate than a univariate statistical analysis for complete structures, e.g., wind turbines, since it can extrapolate the extreme values with better accuracy. This paper uses this ACER2D method to explore a novel approach to estimating the extreme load responses of a 10-MW semi-submersible type floating wind turbine (FWT). Two cases are considered to understand the feasibility of the ACER2D on the extreme load responses. The first case analyses the blade root flap wise bending moment, while the second one analyses the tower bottom fore-aft bending moment. The numerical bending moments used in this study are obtained from the FAST simulation tool (developed by the National Renewable Energy Laboratory) with the load cases simulated at under-rated, rated and above-rated speeds. Then, the ACER2D method is applied to model an extreme response for both these cases for a 5-year return period prediction with a 95 % confidence interval (CI). The proposed methodology permits accurate estimation of the bivariate extreme value. In conclusion, based on the performance of the proposed novel method, the ACER2D method can offer better robust and precise bivariate predictions of the bending moments of the FWT.

Keywords: Floating wind turbine, FAST, ACER2D method, Extreme responses, Bivariate probability distribution.

1. Introduction

Developing more efficient wind turbines is a driving force enabling engineers to achieve the net-zero emissions target 2050 [1]. According to International Electrotechnical Commission (IEC) standards, wind turbines must be designed to operate in the highly stochastic wind and wave environments for at least 20 years [2]. Since both larger and more wind turbines are constructed, especially offshore, it has become extensional to minimise construction, maintenance, and operational costs. Turbines and their components are vulnerable to various cyclic loads such as axial and transverse loading, bending moments and torque. Furthermore, the loads acting on the wind turbines are also influenced by the wind's stochastic behaviours in speed, direction, shear, and vorticity, making extreme load analysis imperative for wind turbines design and operation. Any failure in the turbine system can result in unnecessary downtime, which can be extremely expensive, see [3]-[5]. Despite this, engineers in the 1970s

believed that it was unnecessary to conduct detailed modelling, resulting in the design of wind turbines with huge safety margins. However, this changed with the further development of larger wind turbines as it became more expensive to maintain similar safety margins. On top of that, inaccurate estimation of design loads led to unnecessary failures. These led to an industry revamp, where a better accurate prediction technique was developed by the 1990s using dynamic structural models, turbulence models, aerodynamic models, and control algorithms, see [6].

Two different methods can be applied to evaluate extreme wind turbines loads. The first method involves running a simulation for rare occurrences that leads to a high structural load. In contrast, the second method simulates the wind turbine operating under normal conditions. The results are then extrapolated with a probability distribution, and the extreme tail is analysed, see [7]. The second method is more commonly used as it uses a full statistical distribution instead of an individual event.

ACER univariant analysis of extreme loads is well established and has been a commonly used approach in accessing the extreme loads for wind turbines. However, extending this extreme values analysis from a univariant to a bivariant scenario poses many challenges, especially since there is no direct mapping distribution. Countless attempts have been made to model functions that map dependence between extreme components[47][48]. Nevertheless, there has been minimal success in finding accurate tools to identify the best type of joint distribution for the bivariate extremes of the bivariate data. It is possible to use marginal data sets to estimate the estimated marginal extreme value distribution (EVD), but an actual joint distribution is still a challenge. A very effective technique to cope with such limitations is to use a copula model to characterize a joint distribution structure. The generalized extreme value (GEV) type copula is commonly used this way, but there is no theoretical explanation that explains which should be chosen. The bivariate extreme value copula is no different as countless models could be used, which is made even more challenging because of the properties of dependence. Furthermore, it becomes imperative to observe if a bivariate analysis can be extended accurately to a wind turbine. However, in ACER, it has been shown that it is possible to extend to the bivariate case without needing approximations [49]. A bivariate extreme value copula approach will be applied as a first step in studying a functional depiction of the bivariant ACER surface. This involves combining the univariate ACER functions' asymptotically consistent EVD with the asymmetric logistic (AL) and Gumbel logistic (GL) copula models. This method can additionally validate if the dependence structure of the bivariate EVD can be extended to a wind turbine.

Thus, this paper proposes using the newly developed averaged conditional exceedance rate approach based on two-dimensional design points (ACER2D) instead of traditional one-dimensional characteristic design values. Furthermore, ACER2D is a non-trivial approach compared to the classic method, given that there is a non-linear correlation between different response components. Thus, the proposed method is efficient and reliable in predicting extreme loads and their relationship with one another in a large 10 MW *OO*-Star Floater wind turbine (FWT).

More efficient and reliable estimations of extreme responses will better help predict the effects these loads have on the components allowing the development and implementation of a better design or control system for the FWT. Optimal wind turbine parameters would minimise potential FWT mechanical damage due to excessive environmental loadings [10]. Accurately predicted extreme loads will also allow the components to be more optimally sized. It contributes to more refined designs and lower failure rates, which is particularly important for

the offshore wind industry as it advances the design, manufacturing and deployment of large FWTs (>10 MW) in the coming decade.

2. System description

A 10-MW FWT system [11] is used in this work, which is illustrated in Figure 1. The FWT system will be expounded in two parts in the following sections. Firstly, the reference wind turbine will be described, then the properties of the semi-submersible floater and the mooring system will be introduced.

Figure 1 The LIFES50+ OO-Star Wind Floater Semi 10MW structure [11].

2.1. DTU 10-MW Reference Wind Turbine

The DTU 10-MW reference wind turbine (RWT) [12] is used in this paper, designed from the NREL 5-MW RWT [11]. The wind turbine was designed per the International Electrotechnical Commission (IEC) Class 1A wind regime and is a traditional three-bladed, clockwise rotation-upwind turbine, equipping with a variable speed and collective pitch control system. The DTU 10-MW RWT numerical model has been successfully developed and studied in many academic works, e.g., [13]-[16]. The summary of the DTU 10-MW RWT is shown in Table 1.

Table 1 Key parameters of the DTU 10-MW RWT [11].

Parameter	**Value**
Rating	10-MW
Type	Upwind/3 blades

Control	Variable speed, collective pitch
Drivetrain	Medium-speed, multiple stage gearbox
Cut-in, rated and cut-out wind speed (m/s)	4, 11.4, 25
Minimum and maximum rotor speed (rpm)	6.0, 9.6
Maximum generator speed (rpm)	480
Rotor diameter (m)	178.3
Hub height (m)	119.0
Rotor mass (kg)	227962
Nacelle mass (kg)	446036
Tower mass (kg)	1.257×10^6

2.2. OO-Star Semi-submersible Wind Floater and mooring system

This work uses a semi-submersible floating structure to support the DTU 10-MW RWT. It was introduced by Dr.techn. Olav Olsen AS in the LIFES 50+ project [11]. The floater comprises post-tensioned concrete, hosting a central column with three outer columns. The four columns are mounted on a star-shaped pontoon, where a slab is attached at the bottom. Three catenary mooring lines are used to maintain the floater in position, and in each line, a clumped mass is attached, separating the line into two segments. Greater details of the OO-Star Wind Floater and the mooring system are shown in Table 2 and Table 3, respectively.

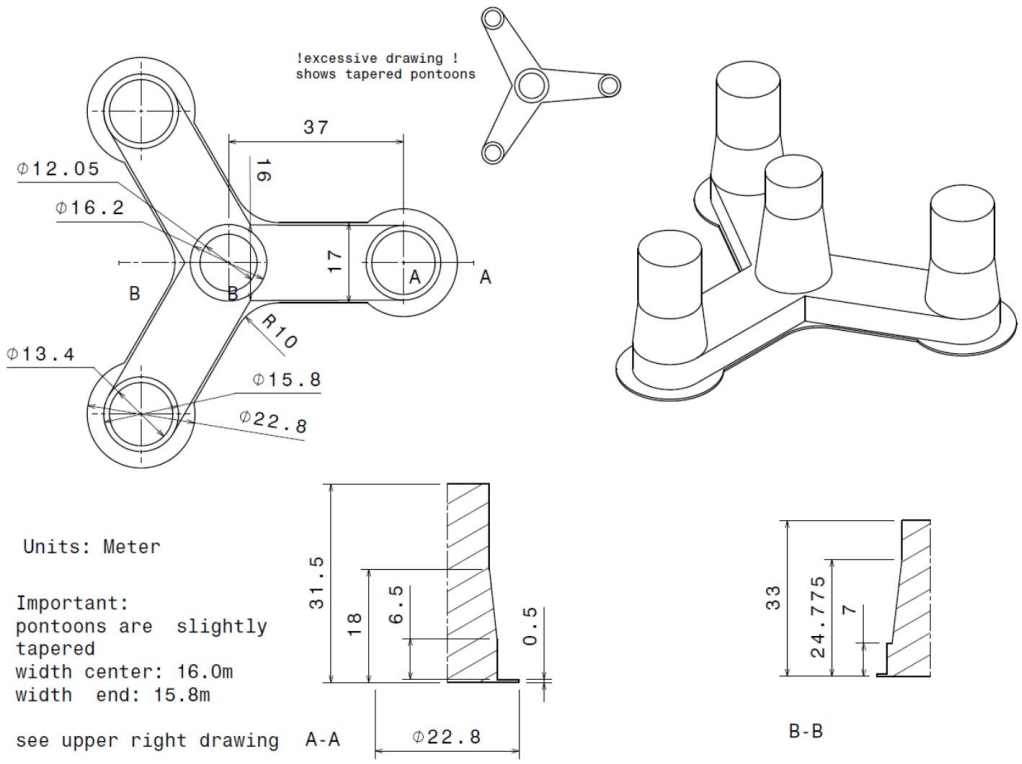

Figure 2 Main dimensions of the OO-Star floater of the LIFES50+ OO-Star Wind Floater Semi 10MW structure [11].

Table 2 The main properties for the LIFES50+ OO-Star Wind Floater Semi 10MW structure wind floater [11].

Parameter	**Value**
Water depth (m)	130
Draft (m)	22
Tower-base interface above mean sea level (m)	11
Displacement (kg)	24158
Overall gravity, including ballast (kg)	21709
Roll and pitch inertia about center of gravity (kg·m^2)	1.4462 x 10^{10}
Yaw inertia about center of gravity (kg·m^2)	1.63 x 10^{10}
Center of gravity height below mean sea level (m)	15.23
Center of buoyancy height below mean sea level (m)	14.236

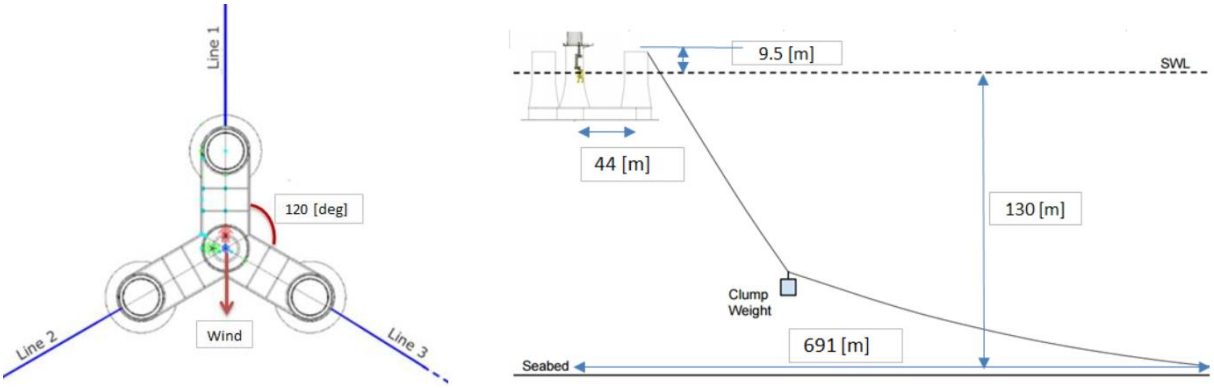

Figure 3 Sketch of the mooring system in the LIFES50+ OO-Star Wind Floater Semi 10MW structure (left: top view; right: side view) [11].

Table 3 The main properties for the mooring system of the LIFES50+ OO-Star Wind Floater Semi 10MW structure [11].

Parameter	**Value**
Radius to anchors from platform centerline (m)	691
Anchor position below MSL (m)	130
Initial vertical position of clump mass below MSL (m)	90.45
Initial radius to clump mass from centerline (m)	148.6
Length of clump mass upper segment (kg)	118
Length of clump mass lower segment (kg)	585
Equivalent weight per length in water (N/m)	3200.6
Extensional stiffness (N/m)	1.506 x 10^9

3. Methodology

This section describes the methodology adopted by authors to address engineering challenges related to safe and reliable design of FWTs (floating wind turbines). Note that the proposed ACER (Average Conditional Exceedance Rate) method along with the FAST simulation tool [40] was already recently successfully used by the authors, see e.g., [40].

3.1. Aero-hydro-elastic-servo dynamic analysis of the 10-MW FWT

FAST (Fatigue, Aerodynamics, Structures and Turbulence) (version8, v8.16.00a-bjj), an open-source WT simulation tool developed by the National Renewable Energy Laboratory (NREL), is utilized in this work for the fully coupled aero-hydro-elastic-servo dynamic analysis for the 10-MW FWT [46]. The FAST code couples together five computer codes: AeroDyn [17], HydroDyn [18], ServoDyn, and MoorDyn [19], to account for the aerodynamic loads on rotor blades, hydrodynamic loads on floaters, control dynamics, structural dynamics and mooring system dynamics. In addition, FAST provides the interface for reading the time-varying stochastic wind for time-domain simulations. The FAST simulation tool has been successfully used in other well-known projects such as OC3: Offshore Code Comparison Collaboration [20] and OC4: IEA Task Wind 30 [21], and its modelling capability has been authenticated using multiple floating structures in the Netherlands [22].

3.2. Extreme value prediction by ACER1D and ACER2D methods

ACER1D method

Various statistical methods have been used to approximate the extreme value distribution of a recorded time series in its tail. Examples of the extreme value methods used in the study of wind turbines include an estimation of extreme structural responses in floating vertical axis wind turbines, see [23] and extreme responses due to wave nonlinearity on a semi-submersible floating wind turbine, see [10].

The ACER method used in this paper as in [24]-[30], [38]-[45] has numerous advantages when estimating extreme values from a recorded time series. One of these includes the ability to identify the effect of dependency between the data of the time series on the extreme value distribution. Also, the whole time series can be used as input data without de-clustering (i.e., no requirement to use independent data). However, the most prominent feature of the ACER method is its ability to provide a non-parametric depiction of the extreme value distribution inherent in the data. The ACER1D values are calculated in this paper using the ACER1D method from [8][9] to create a functional form of the Asymmetric-logistic and Gumbel-logistic dependence function to be compared against the ACER2D function.

ACER2D method

Now, the 2D (bivariate) Average Conditional Exceedance Rate, or briefly ACER2D method, has been applied to analyse FWT blade root and tower bottom bending moment due to environmental wind and wave loads. A brief introduction of the bivariate ACER2D method is outlined below; see [61]-[64] for more details. Note that both of the stochastic response processes (blade root and tower bottom bending moments) mentioned above, are time synchronous. The latter is undoubtedly beneficial for coupling effects and bivariate statistics

study.

This paper studies a bivariate stochastic process $Z(t) = (X(t), Y(t))$, having two scalar processes $X(t), Y(t)$, simulated synchronously, over a time span $(0, T)$. The bivariate data points $(X_1, Y_1), \dots, (X_N, Y_N)$ correspond to equidistant time instants $t_1, \dots, t_N$.

The joint CDF (cumulative distribution function) $P(\xi, \eta) := \text{Prob}\left(\hat{X}_N \le \xi, \hat{Y}_N \le \eta\right)$ of the maxima vector $\left(\hat{X}_N, \hat{Y}_N\right)$, with $\hat{X}_N = \max\{X_j\,; j = 1, \dots, N\}$, and $\hat{Y}_N = \max\{Y_j\,; j = 1, \dots, N\}$ is introduced. In this paper, ξ and η are blade root and tower bottom mooring bending moments, M_1 and M_3 in **Figure 5** respectively.

Next, the non-exceedance event is introduced: $\mathcal{C}_{kj}(\xi, \eta) := \{X_{j-1} \le \xi, Y_{j-1} \le \eta, \dots, X_{j-k+1} \le \xi, Y_{j-k+1} \le \eta\}$ for $1 \le k \le j \le N + 1$. Based on the definition of the joint CDF $P(\xi, \eta)$

$$\begin{aligned} P(\xi,\eta) &= \text{Prob}\left(\mathcal{C}_{N+1,N+1}(\xi,\eta)\right) \\ &= \text{Prob}\left(X_N \le \xi, Y_N \le \eta \mid \mathcal{C}_{NN}(\xi,\eta)\right) \cdot \text{Prob}\left(\mathcal{C}_{NN}(\xi,\eta)\right) \\ &= \prod_{j=2}^{N} \text{Prob}\left(X_j \le \xi, Y_j \le \eta \mid \mathcal{C}_{jj}(\xi,\eta)\right) \cdot \text{Prob}\left(\mathcal{C}_{22}(\xi,\eta)\right) \end{aligned} \tag{1}$$

The CDF $P(\xi, \eta)$ can be expressed as in [31]-[34]

$$P(\xi,\eta) \approx \exp\left\{-\sum_{j=k}^{N}\left(\alpha_{kj}(\xi;\eta) + \beta_{kj}(\eta;\xi) - \gamma_{kj}(\xi,\eta)\right)\right\} \tag{2}$$

for a suitably large conditioning level parameter k, and large ξ and η with $\alpha_{kj}(\xi;\eta) := \text{Prob}\left(X_j > \xi \mid \mathcal{C}_{kj}(\xi,\eta)\right)$, $\beta_{kj}(\eta;\xi) := \text{Prob}\left(Y_j > \eta \mid \mathcal{C}_{kj}(\xi,\eta)\right)$, $\gamma_{kj}(\xi,\eta) := \text{Prob}\left(X_j > \xi, Y_j > \eta \mid \mathcal{C}_{kj}(\xi,\eta)\right)$.

Next, the k-th order bivariate average conditional exceedance rate (ACER2D) functions can be introduced

$$\mathcal{E}_k(\xi,\eta) = \frac{1}{N-k+1}\sum_{j=k}^{N}\left(\alpha_{kj}(\xi;\eta) + \beta_{kj}(\eta;\xi) - \gamma_{kj}(\xi,\eta)\right) \tag{3}$$

for $k = 1, 2, \dots$; when $N \gg k$

$$P(\xi,\eta) \approx \exp\{-(N-k+1)\mathcal{E}_k(\xi,\eta)\}\,; \text{ for large } \xi \text{ and } \eta. \tag{4}$$

From Eq. (4), it follows that an accurate estimate of the bivariate CDF $P(\xi, \eta) = P(\xi, \eta)$ relies on the equally accurate estimation of ACER2D functions $\mathcal{E}_k$.

3.3. Load cases and environmental conditions

The environmental data (wind and wave data) used in this paper are established based on hindcast data from an offshore site in the Northern North Sea from 2001 to 2010. The long-term joint wind and wave distribution were developed in [35], which considers a one-hour mean wind speed at the position that is 10 meters above the sea level (U_{10}), wave spectral peak period (T_p) and the significant wave height (H_s). The joint distribution of U_{10}, H_s and T_p is expressed as below:

$$f_{U_{10},H_s,T_p}(u,h,t) = f_{U_{10}}(u) \cdot f_{H_s|U_{10}}(h|u) \cdot f_{T_p|U_{10},H_s}(t|u,h) \quad (5)$$

where $f_{U_{10}}(u)$, $f_{H_s|U_{10}}(h|u)$ *and* $f_{T_p|U_{10},H_s}(t|u,h)$ represents the marginal distribution of U_{10}, the conditional distribution of H_s for given U_{10} and the conditional distribution of T_p for given U_{10} and H_s. Figure 4 illustrates in situ H_s, T_p scattered diagram, used to assign probabilities to individual sea states.

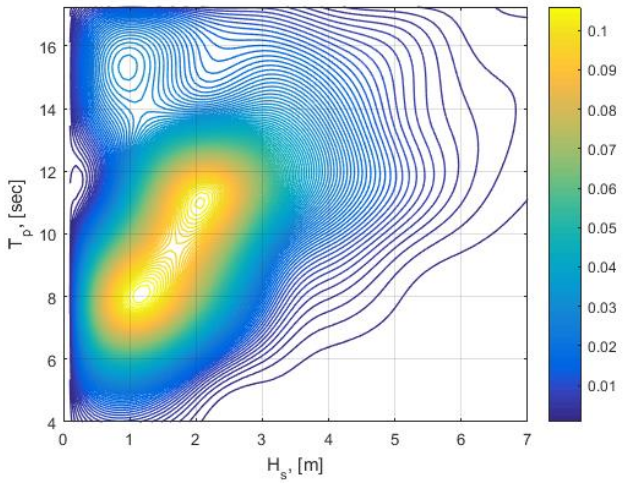

Figure 4 An example of in situ H_s, T_p scattered diagram, used to assign probabilities to individual sea states.

Table 4 Load cases for numerical simulations.

Load cases	U_w (m/s)	T_I	H_s (m)	T_p (s)	Samples	Simulation length (s)
LC1	8	0.1740	1.9	9.7	20	4000
LC2	12	0.1460	2.5	10.1	20	4000
LC3	16	0.1320	3.2	10.7	20	4000

Three representative load cases with a high probability of occurrence in the normal operating conditions are used in the present work and listed in Table 4. The mean wind speed selected to be used in this paper is based on the turbines operating ranges (wind speeds ranging within the cut-in, rated and cut-out zones) with an increment size of 4 m/s. The most probable wave height

and spectra peak period in each wind speed condition is selected based on the joint distribution expressed in Eq. (5).

The turbulent wind and irregular waves are modelled, and they are considered to be directionally aligned in all the load cases. The normal turbulence and normal wind profile models are employed, and wind turbine Class C is applied. The wind power-law formulation is used to model the wind speed profile, as represented below:

$$U_w(z) = U_{hub}\,(\frac{\mathrm{Z}}{Z_{hub}})^{\alpha} \qquad (6)$$

where $U_w(z)$ is the mean wind speed at the height z above the still water level, u_{hub} represents the mean wind speed at the hub height, z_{hub} denotes the hub height above the still water level and is 119 m for the 10-MW FWT. α is the power-law exponent, and it is taken as 0.14 for offshore locations based on the recommendation in IEC 61400-3-2, see [36].

The Kaimal turbulence model is used to generate the three-dimensional turbulent wind fields, simulated using a stochastic turbulent-wind simulator, Turbsim [37]. Time-varying irregular waves are generated using the JONSWAP (Joint North Sea Wave Project) spectrum according to the specified H_s and T_p. Detailed descriptions for the models of turbulent wind and irregular waves can be found in IEC 61400-3-2 [36].

For the three environmental conditions, 20 different random samples of wind and wave are applied for each sea state. Each simulation lasts 4000s, where the first 400s is removed to reduce the transient effect induced by the wind turbine start-up. Therefore, 1-h data in each simulation is formed and is used for extreme value analysis in this work. The results shown in this work are based on the average of 20 1-h simulations to reduce the stochastic variability.

4. Results and discussions

This paper presents the methodology for estimating the DTU 10-MW RWT-OO-Star's extreme loads during operating conditions. The empirical data is based on accurate numerical simulations using a FAST model as presented in Section 3.1. The ACER2D (bivariate averaged conditional exceedance rate) method is presented in Section 3.2.

The loads at the two measurement points presented in **Figure 5** are considered. These are the blade 1 root flapwise bending moment (RootMyb1) and tower bottom fore-aft bending moment (TwrBsMyt).

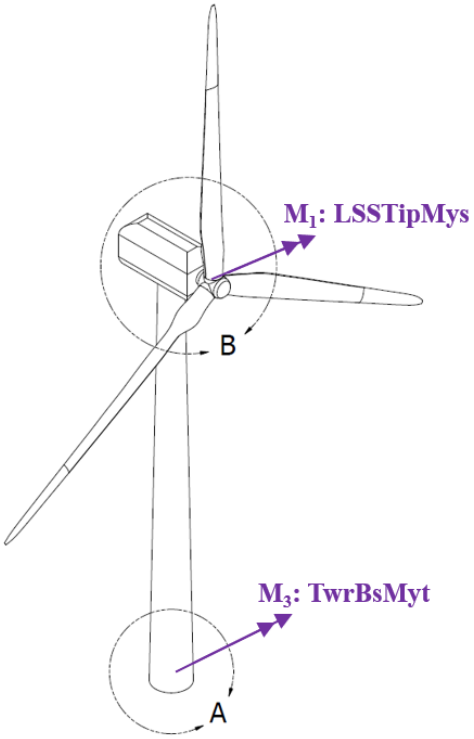

Figure 5 Location of points where bending moments are measured.

4.1. Power Spectral Density based on time responses

Figure 7 of M_1, M_3. It is seen that there are PSD (Power Spectral Density) peaks at the frequencies *f* at 3P, 6P and 9P as observed in Figure 6. This information should be reflected in the ACER functions' choice of conditioning level k.

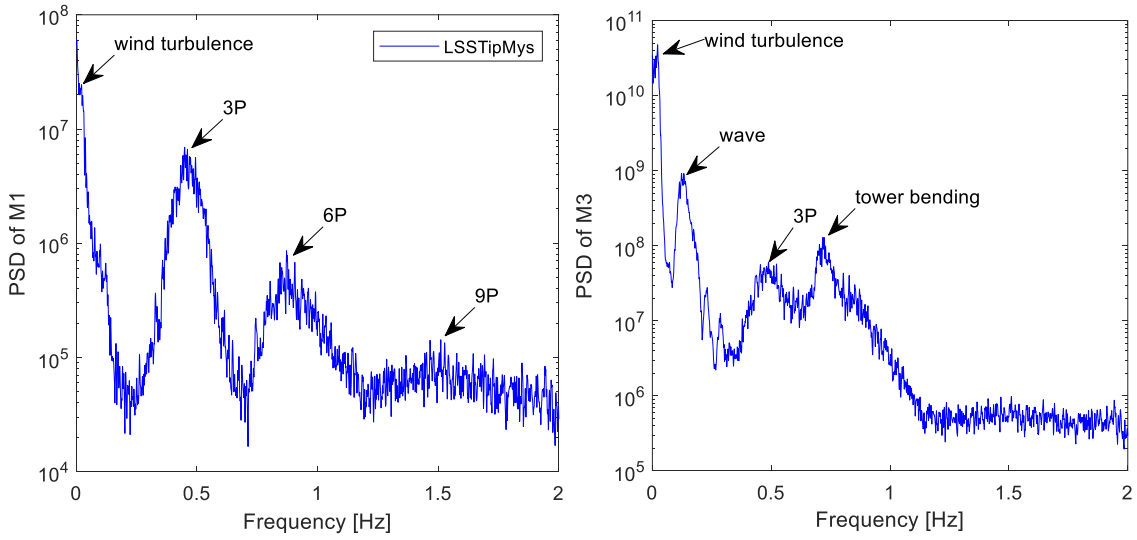

Figure 7 PSD of LSSTipMys – M1 and TwrBsMyt – M3

4.2. Extreme responses: univariate and bivariate analysis

This section presents statistical analysis results for M_1 and M_3 bending moments using the univariate and bivariate methods, i.e., ACER1D and ACER2D, respectively. The focus is on accurate predicting extreme response, which is vital for safety and reliability at the design stage. The conditioning level *k* is set to be 10, as it was observed that ACER functions have converged at that level in the distribution tail.

Figure 8 presents univariate extreme response 5-year return period prediction with 95 % confidence interval (CI); the 1-year return period is chosen purely as an example. The predicted extreme probability level corresponds to 5-year return period.

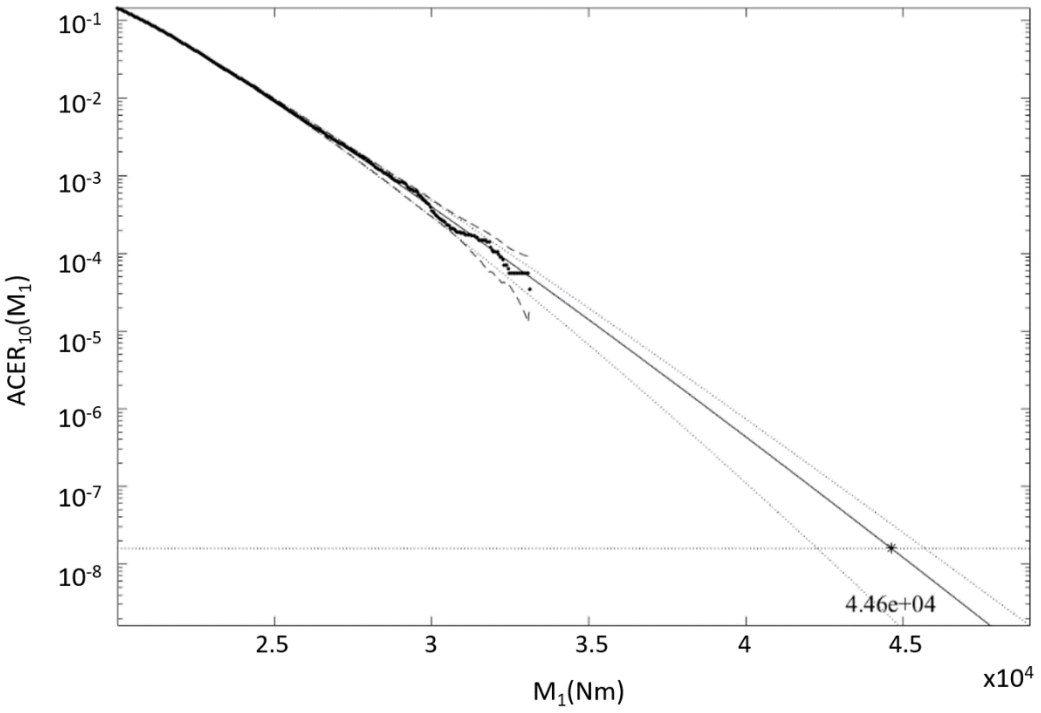

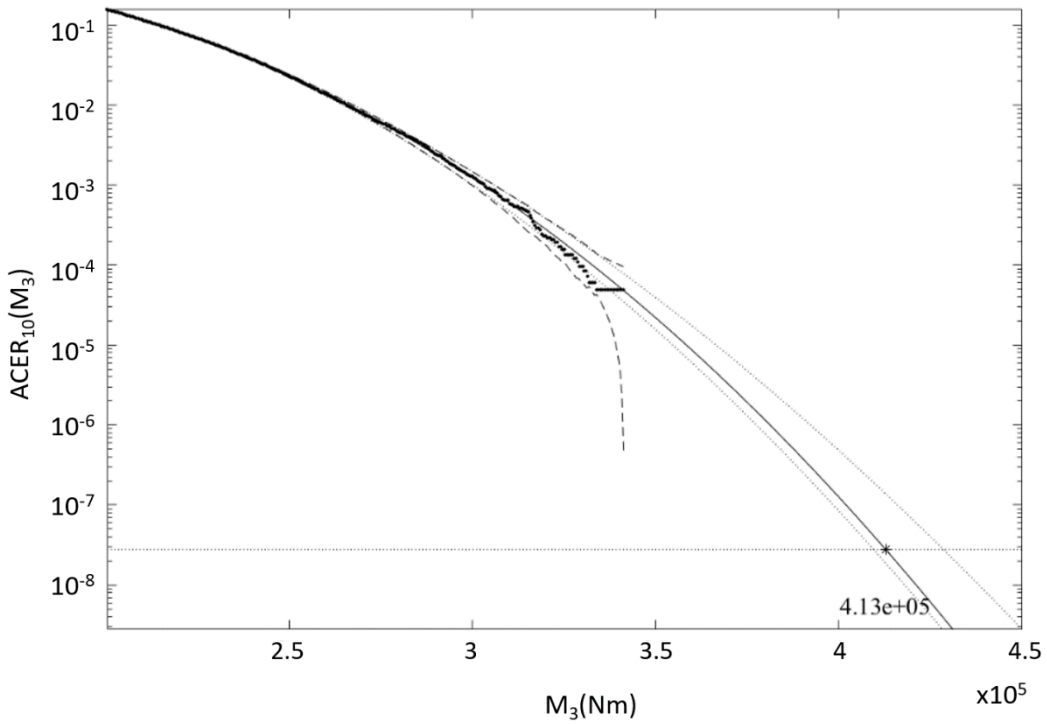

Figure 8 Univariate ACER1D extreme response 5-year prediction with 95% CI (dotted lines). Top: RootMyb1 – M_1; Bottom: TwrBsMyt – M_3; decimal log scale.

Figure 9 presents the phase space of responses M_1 over M_3, along with the bivariate empirical ACER2D function $\hat{\mathcal{E}}_k$. It is clearly seen that there is a non-linear correlation between responses M_1 and M_3. The bivariate empirical ACER2D surface, $\hat{\mathcal{E}}_k$ obviously marginally corresponds to univariate ACER1D functions presented in Figure 8.

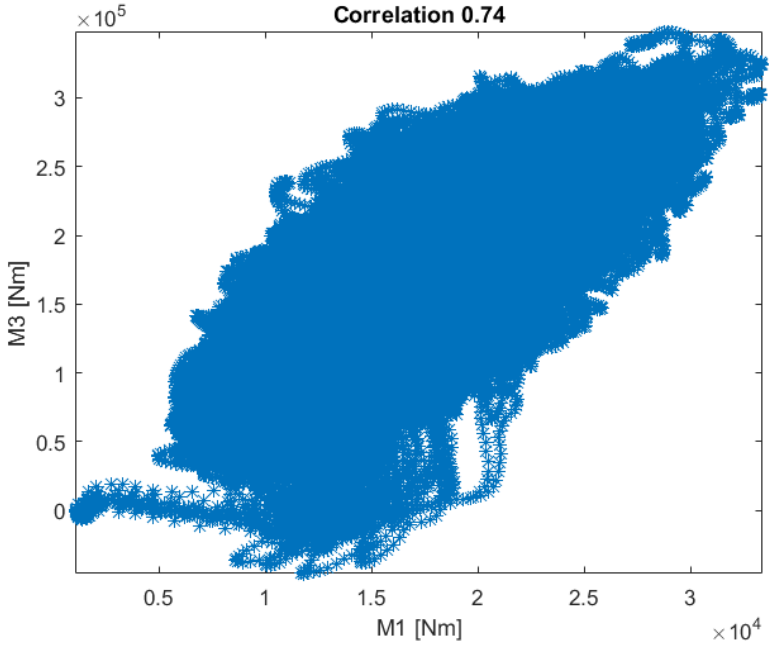

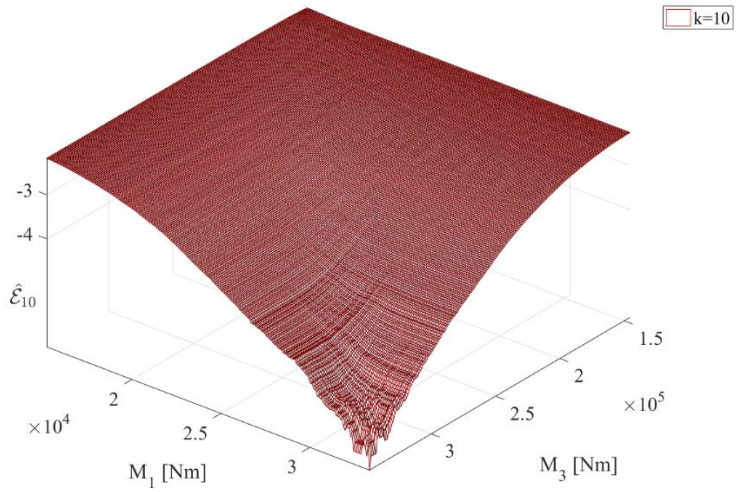

Figure 9 Top: phase space, response M_1 vs M_3; Bottom: bivariate empirical ACER2D function $\hat{\mathcal{E}}_k$, decimal log scale.

Figure 10 presents ACER2D fit to the empirical data along with the bivariate predicted contours with return periods in years (lower figure). Figure 10 presents contour lines for the optimized Asymmetric logistic (AL) $\mathcal{A}_k(M_1, M_3)$ and optimized Gumbel logistic (GL) $\mathcal{G}_k(M_1, M_3)$ models, optimally matched to the corresponding empirical bivariate ACER2D function $\hat{\mathcal{E}}_k(M_1, M_3)$, $k = 10$, see [31]-[34] for GL and AL definitions. The contour lines negative labelling numbers in Figure 10 indicate decimal logarithmic scale probability levels of $P(M_1, M_3)$. Figure 10 clearly shows that the empirical bivariate ACER2D surface $\hat{\mathcal{E}}_{10}$ well captures the strong correlation between load/response components. The optimized models $\mathcal{G}_{10}$ and $\mathcal{A}_{10}$ exhibit smooth contours along with matching ACER2D empirical contours. The later models may be better suited for bivariate extreme value distributions response processes. Figure 10 shows good agreement between the estimated optimized AL and GL surfaces and the bivariate ACER2D surface. This means that the correlation between responses M_1 vs M_3 is a crucial non-negligible factor influencing the shape of the bivariate contour lines.

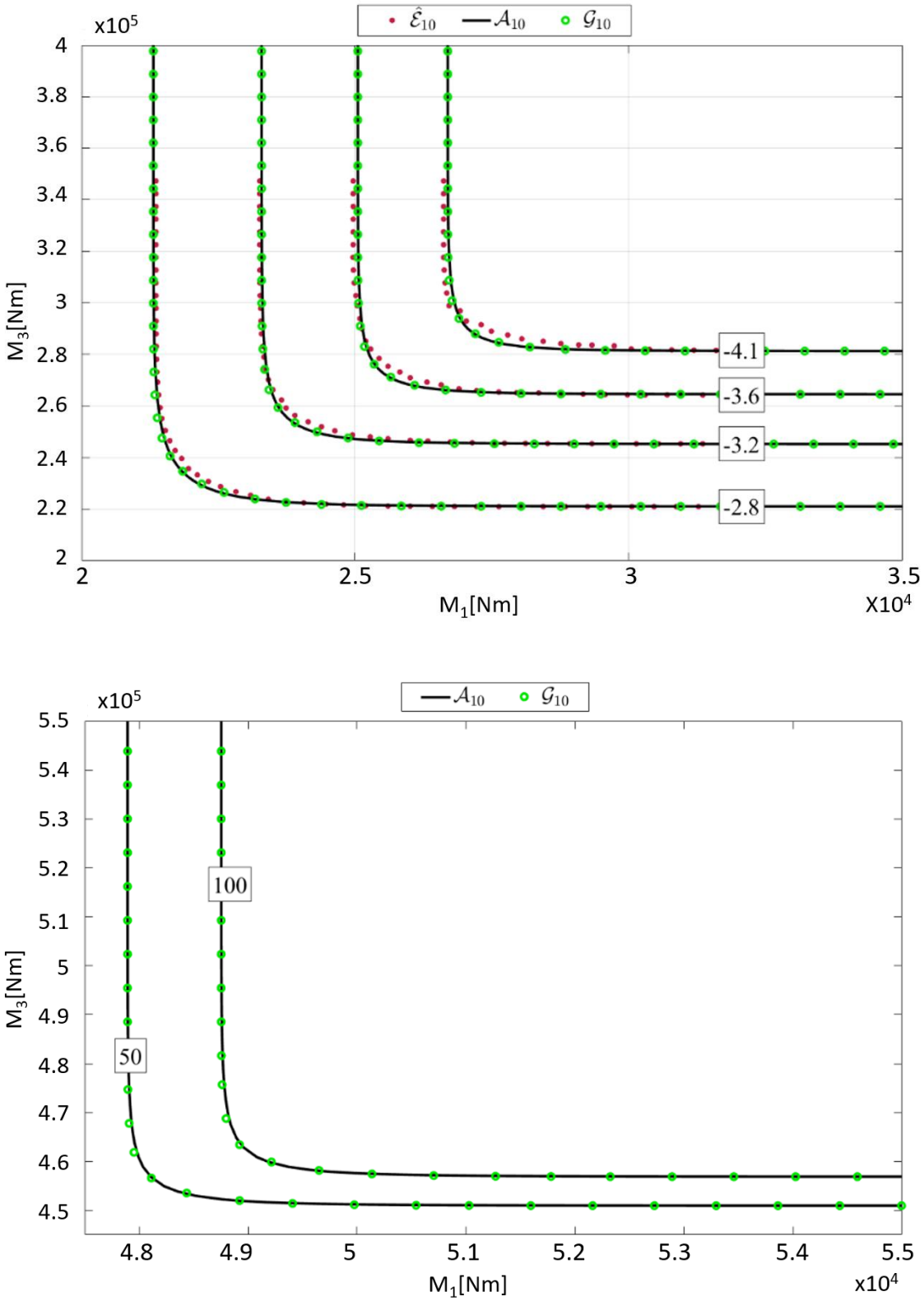

Figure 10 Top: ACER2D fit to empirical data; Bottom: predicted bivariate contours with return periods in years.

The lowest probabilities in Figure 9 and Figure 10 correspond to the value N^{-1} where N is the number of equidistant time points in the studied time series. Figure 8 (bottom) presents the predicted bivariate contours with 50- and 100-years corresponding return periods. Note that the return period of a few years is quite long compared to the short duration of the analysed

measured record. As seen from Figure 10 (bottom), the fitted lines match the empirical data well, highlighting the accuracy of the ACER method. Further, the ACER method is efficient as it requires only 20 1-hour realisations to generate accurate results.

Figure 11 shows that the univariate design point lies outside the safe 50-year zone (dashed area) and is outside the 2D design zone. This means that the 1D method is not conservative.

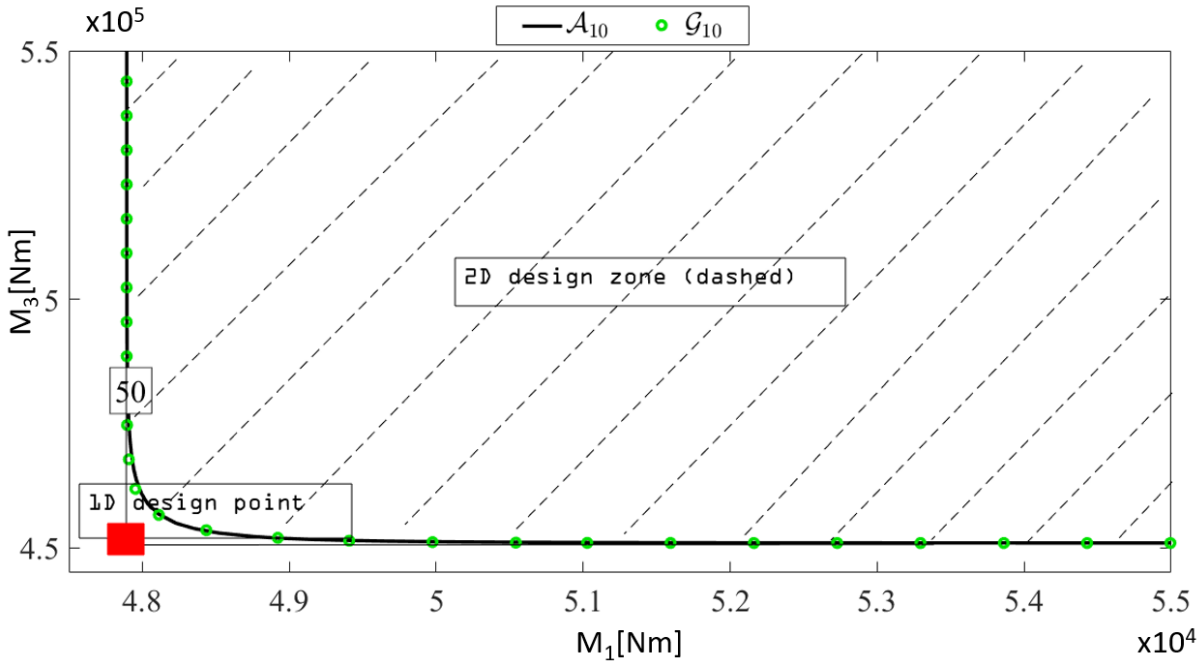

Figure 11 Design safe zone (dashed) due to bivariate analysis, versus univariate design point, based on Figure 10. Asymmetric logistic $\mathcal{A}_k(M_1, M_3)$ 50-year contour line.

Table 5 presents 50- and 100-year return period ACER1D response predictions in meters.

Table 5 50- and 100-year return period response ACER1D predictions

	50 yr	**100 yr**
M_1 (Nm)	4.8 x 10^4	4.9 x 10^4
M_3 (Nm)	4.5 x 10^5	4.6 x 10^5

5. Conclusions

A new approach that is based on a 2D design point instead of the traditional 1D characteristic design values has been examined on the DTU 10-MW FWT. The proposed methodology provides an accurate bivariate extreme value prediction, utilizing all available data efficiently. Based on the overall performance of the proposed method, it was concluded that the ACER2D method could incorporate environmental input and provide a more robust and accurate bivariate prediction based on proper numerical simulations. The method uses only a relatively small amount of data to provide reasonable predictions with long return periods.

The FWT blade root and tower bottom bending moments due to environmental wind and wave loads were studied for three operating conditions of mean wind speeds of 8, 12 and 16 m/s. The

bivariate ACER2D method was briefly described and applied to account for the coupled load effects, namely dynamic moment and force simulated synchronously in time. Bivariate extreme value distribution low probabilities (or equivalently high quantiles) contours were estimated by adopting various bivariate copula models. Potential outliers present in the data set are also well managed by being neglected in the distribution tail through the proposed extrapolation and copula fit technique.

Regarding the safety and reliability of FWT operations, the multivariate analysis is a more proper approach than the classic univariate approach. The presented technique has the following advantages:

- Unlike IFORM/ SORM, the ACER2D method does not simplify model nonlinearities.
- Various kinds of coupled data can be studied: measured or numerically simulated.
- Clustering effects can be accounted for.
- The ACER2D method provides a more conservative prediction of the extreme values, especially in the regions where the variables are more strongly coupled together, i.e., at the value predicted by the 1D method.
- The ACER2D method may provide an efficient way of identifying practical design appropriate bivariate copula models.

The described approach may be used at the design stage of a large FWT to provide the opportunity of defining FWT parameters that would minimize extreme loads and potential damages. It is also noted that the study is limited to the quality of the data itself. This limitation applies for any type of statistical method.

References

[1] International Energy Agency. (2020). World energy outlook 2020. OECD Publishing.

[2] Veers, P., Butterfield, S. (2001). Extreme load estimation for wind turbines-issues and opportunities for improved practice. In 20th 2001 ASME Wind Energy Symposium (p. 44).

[3] Igba, J., Alemzadeh, K., Durugbo, C., Henningsen, K. (2015). Performance assessment of wind turbine gearboxes using in-service data: Current approaches and future trends. Renewable and Sustainable Energy Reviews, 50, 144-159.

[4] Irena, I. R. E. A. (2012). Renewable energy technologies: Cost analysis series. Wind Power.

[5] Sheng, S. (2012). Wind turbine gearbox condition monitoring round robin study-vibration analysis (No. NREL/TP-5000-54530). National Renewable Energy Lab.(NREL), Golden, CO (United States).

[6] Veers, P. S., Winterstein, S. R. (1998). Application of measured loads to wind turbine fatigue and reliability analysis.

[7] Dimitrov, N. (2016). Comparative analysis of methods for modelling the short-term probability distribution of extreme wind turbine loads. Wind Energy, 19(4), 717-737.

[8] Næss, A., Gaidai, O. (2009). Estimation of extreme values from sampled time series. Structural Safety, 31(4), 325-334.

[9] Naess, A., Gaidai, O., Batsevych, O. (2010). Prediction of extreme response statistics of narrow-band random vibrations. Journal of Engineering Mechanics, 136(3), 290-298.

[10] Xu, K., Zhang, M., Shao, Y., Gao, Z., Moan, T. (2019). Effect of wave nonlinearity on fatigue damage and extreme responses of a semi-submersible floating wind turbine. Applied Ocean Research, 91, 101879. doi: 10.1016/j.apor.2019.101879
[11] Yu, W., Müller, K., Lemmer, F., Bredmose, H., Borg, M., Sanchez, G., Landbo, T. (2017). Public Definition of the Two LIFES50+ 10MW Floater Concepts.". *LIFES50+ Deliverable*, *4*.
[12] Bak, C., Zahle, F., Bitsche, R., Kim, T., Yde, A., Henriksen, L., Hansen, M.H., Blasques, J.P.A.A., Gaunaa, M.A., Natarajan, M. H. (2013). The DTU 10-MW reference wind turbine, Danish wind power Research 2013.
[13] Muggiasca, S., Taruffi, F., Fontanella, A., Di Carlo, S., Giberti, H., Facchinetti, A., Belloli, M. (2021). Design of an aeroelastic physical model of the DTU 10MW wind turbine for a floating offshore multipurpose platform prototype. Ocean Engineering, 239, 109837. doi: 10.1016/j.oceaneng.2021.109837
[14] Yu, Z., Amdahl, J., Rypestøl, M., Cheng, Z. (2022). Numerical modelling and dynamic response analysis of a 10 MW semi-submersible floating offshore wind turbine subjected to ship collision loads. Renewable Energy, 184, 677-699.
[15] Wang, S., Moan, T., Jiang, Z. (2022). Influence of variability and uncertainty of wind and waves on fatigue damage of a floating wind turbine drivetrain. Renewable Energy, 181, 870-897.
[16] Hu, R., Le, C., Gao, Z., Ding, H., Zhang, P. (2021). Implementation and evaluation of control strategies based on an open controller for a 10 MW floating wind turbine. Renewable Energy, 179, 1751-1766.
[17] Moriarty, P. J., Hansen, A. C. (2005). *AeroDyn theory manual* (No. NREL/TP-500-36881). National Renewable Energy Lab., Golden, CO (US).
[18] Jonkman, J. M., Robertson, A. N., Hayman, G. J. (2014). HydroDyn user's guide and theory manual. *National Renewable Energy Laboratory*.
[19] Hall M. MoorDyn user's guide. Orono, ME: Department of Mechanical Engineering, University of Maine, 2015.
[20] Jonkman, J., Musial, W. (2010). Offshore code comparison collaboration (OC3) for IEA Wind Task 23 offshore wind technology and deployment (No. NREL/TP-5000-48191). National Renewable Energy Lab.(NREL), Golden, CO (United States).
[21] Robertson, A., Jonkman, J., Musial, W., Popko, W., Vorpahl, F. (2014). IEA Wind Task 30 Offshore Code Comparison Collaboration Continued.
[22] Coulling, Alexander Goupee, Andrew Robertson, Amy Jonkman, Jason Dagher, Habib. (2013). Validation of a FAST semi-submersible floating wind turbine numerical model with DeepCwind test data. Journal of Renewable and Sustainable Energy. 5. 10.1063/1.4796197.
[23] Cheng, Z., Madsen, H. A., Chai, W., Gao, Z., Moan, T. (2017). A comparison of extreme structural responses and fatigue damage of semi-submersible type floating horizontal and vertical axis wind turbines. Renewable Energy, 108, 207-219.
[24] Naess, A., Gaidai, O., Batsevych, O. (2010). Prediction of extreme response statistics of narrow-band random vibrations. Journal of engineering mechanics, 136(3), 290-298.
[25] Naess, A., Gaidai, O. (2008). Monte Carlo methods for estimating the extreme response of dynamical systems. Journal of Engineering Mechanics, 134(8), 628-636.
[26] Xu, X. S., Gaidai, O., Karpa, O., Wang, J. L., Ye, R. C., Cheng, Y. (2021). Wind Farm Support Vessel Extreme Roll Assessment While Docking in the Bohai Sea. China Ocean Engineering, 35(2), 308-316.
[27] Zhao, Y., Liao, Z., Dong, S. (2021). Estimation of characteristic extreme response for mooring system in a complex ocean environment. Ocean Engineering, 225, 108809.

[28] Galambos, J., Marci, N. (1999). Classical extreme value model and prediction of extreme winds. Journal of Structural Engineering, 125(7), 792-794.
[29] Naess, A., Moan, T. (2013). Stochastic dynamics of marine structures. Cambridge University Press.
[30] Naess, A., Stansberg, C. T., Gaidai, O., Baarholm, R. J. (2009). Statistics of extreme events in airgap measurements. Journal of offshore mechanics and Arctic engineering, 131(4).
[31] Naess, A, Karpa, O. (2015), "Statistics of bivariate extreme wind speeds by the ACER2D method", J. Wind Eng. and Ind. Aerodyn. Vol 139, pp.82–88.
[32] Karpa, O., and Naess, A. (2015), "Statistics of Extreme Wind Speeds and Wave Heights by the Bivariate ACER2D Method", Journal of Offshore Mechanics and Arctic Engineering, Vol 137(2).
[33] Gaidai, O, and Storhaug, G, and Naess, A. (2016) "Extreme large cargo ship panel stresses by bivariate ACER2D method", Ocean Engineering, Vol. 127, pp. 368-386.
[34] Jian, Z, Gaidai, O, Gao, J. (2018), "Bivariate Extreme Value Statistics of Offshore Jacket Support Stresses in Bohai Bay", Journal of Offshore Mechanics and Arctic Engineering, Vol 140 (4).
[35] Li, L., Gao, Z., Moan, T. (2013). Joint environmental data at five European offshore sites for design of combined wind and wave energy concepts. In 32nd International Conference on Ocean, Offshore, and Arctic Engineering, no. OMAE2013-10156.
[36] IEC 61400-3-2 (2019). Part 3-2: Design requirements for floating offshore wind turbines.
[37] Jonkman, B. J. (2009). TurbSim user's guide: Version 1.50 (No. NREL/TP-500-46198). National Renewable Energy Lab.(NREL), Golden, CO (United States).
[38] Gaidai, O., Ji, C., Kalogeri, C., Gao, J. (2017). SEM-REV energy site extreme wave prediction, Renewable Energy, Vol 101, pp. 894-899.
[39] X. Xu, O. Gaidai, O. Karpa, J. Wang, R. Ye, Y. Cheng, (2021), Wind Farm Support Vessel Extreme Roll Assessment While Docking in the Bohai Sea, China Ocean Engineering, Vol 35 (2), pp. 308-316.
[40] Xu, X., Gaidai, O., Naess, A., Sahoo, P., (2020), Extreme loads analysis of a site-specific semi-submersible type wind turbine, Ships and Offshore structures, DOI: 10.1080/17445302.2020.1733315.
[41] Bak, C., Zahle, F., Bitsche, R., Kim, T., Yde, A., Henriksen, L.C., Hansen, M.H., Blasques, J.P.A.A., Gaunaa, M. and Natarajan, A., 2013. The DTU 10-MW reference wind turbine. In Danish Wind Power Research 2013.
[42] Naess, A, Karpa, O. (2015), "Statistics of bivariate extreme wind speeds by the ACER2D method", J. Wind Eng. and Ind. Aerodyn. Vol 139, pp.82–88.
[43] Karpa, O., and Naess, A. (2015), "Statistics of Extreme Wind Speeds and Wave Heights by the Bivariate ACER2D Method", Journal of Offshore Mechanics and Arctic Engineering, Vol 137(2).
[44] Gaidai, O, and Storhaug, G, and Naess, A. (2016) "Extreme large cargo ship panel stresses by bivariate ACER2D method", Ocean Engineering, Vol. 127, pp. 368-386.
[45] Jian, Z, Gaidai, O, Gao, J. (2018), "Bivariate Extreme Value Statistics of Offshore Jacket Support Stresses in Bohai Bay", Journal of Offshore Mechanics and Arctic Engineering, Vol 140 (4).
[46] Jonkman, J. M., & Buhl, M. L. (2005). FAST users guide NREL/EL-500-38230. National Renewable Energy Laboratory, Tech. Rep.
[47] Coles, S. G., and Tawn, J. A., 1991, “Modeling Extreme Multivariate Events,” J. R. Stat. Soc. B, 53(2), pp. 377–392.
[48] Coles, S. G., and Tawn, J. A., 1994, “Statistical Methods for Multivariate Extremes: An Application to Structural Design,” J. R. Stat. Soc. C, 43(1), pp. 1–48.

[49] Naess, A., 2011, “A Note on the Bivariate ACER Method,” Department of Mathematical Sciences, Norwegian University of Science and Technology, Trondheim, Preprint Statistics No. 01/2011.